School of Natural Sciences and Mathematics
William B. Hanson Center for Space Sciences

Coherently Modulated Whistler Mode Waves Simultaneously Observed over Unexpectedly Large Spatial Scales

UT Dallas Author(s):
Lunjin Chen

Citation:
Li, Jinxing, Jacob Bortnik, Wen Li, Richard M. Thorne, et al. 2017. "Coherently modulated whistler mode waves simultaneously observed over unexpectedly large spatial scales." Journal of Geophysical Research-Space Physics 122(2): 1871-1882, doi:10.1002/2016JA023706

AGU PUBLICATIONS

JGR

Journal of Geophysical Research: Space Physics

RESEARCH ARTICLE

10.1002/2016JA023706

Key Points:
- Coherently modulated whistler mode waves are continuously observed over unexpectedly large spatial scales up to 4.3 R_E
- Wave coherence depends on frequency and changes with different spacecraft spatial configurations
- The sources of coherently modulated waves in each phase are investigated by cross correlations and electron anisotropy

Correspondence to:
J. Li,
jli@atmos.ucla.edu

Citation:
Li, J., et al. (2017), Coherently modulated whistler mode waves simultaneously observed over unexpectedly large spatial scales, *J. Geophys. Res. Space Physics*, *122*, 1871–1882, doi:10.1002/2016JA023706.

Received 18 NOV 2016
Accepted 3 FEB 2017
Accepted article online 5 FEB 2017
Published online 17 FEB 2017

Coherently modulated whistler mode waves simultaneously observed over unexpectedly large spatial scales

Jinxing Li[1], Jacob Bortnik[1], Wen Li[1,2], Richard M. Thorne[1], Qianli Ma[1], Xiangning Chu[1], Lunjin Chen[3], Craig A. Kletzing[4], William S. Kurth[4], George B. Hospodarsky[4], John Wygant[5], Aaron Breneman[5], and Scott Thaller[5]

[1]Department of Atmospheric and Oceanic Sciences, University of California, Los Angeles, California, USA, [2]Center for Space Physics, Boston University, Boston, Massachusetts, USA, [3]W. B. Hanson Center for Space Sciences, Department of Physics, University of Texas at Dallas, Richardson, Texas, USA, [4]Department of Physics and Astronomy, University of Iowa, Iowa City, Iowa, USA, [5]School of Physics and Astronomy, University of Minnesota, Minneapolis, Minnesota, USA

Abstract Utilizing simultaneous twin Van Allen Probes observations of whistler mode waves at variable separations, we are able to distinguish the temporal variations from spatial variations, determine the coherence spatial scale, and suggest the possible mechanism of wave modulation. The two probes observed coherently modulated whistler mode waves simultaneously at an unexpectedly large distance up to ~4.3 R_E over 3 h during a relatively quiet period. The modulation of 150–500 Hz plasmaspheric hiss was correlated with whistler mode waves measured outside the plasmasphere across 3 h in magnetic local time and 3 L shells, revealing that the modulation was temporal in nature. We suggest that the coherent modulation of whistler mode waves was associated with the coherent ULF waves measured over a large scale, which modulate the plasmaspheric density and result in the modulation of hiss waves via local amplification. In a later period, the 500–1500 Hz periodic rising-tone whistler mode waves were strongly correlated when the two probes traversed large spatial regions and even across the plasmapause. These periodic rising-tone emissions recurred with roughly the same period as the ULF wave, but there was no one-to-one correspondence, and a cross-correlation analysis suggests that they possibly originated from large L shells although the actual cause needs further investigation.

1. Introduction

Whistler mode waves are right-hand polarized electromagnetic waves that are often observed in space plasmas. Whistler mode chorus is a discrete and coherent emission, observed in the low-density region exterior to the plasmapause [*Li et al.*, 2011a] in two distinct frequency bands above and below 0.5 f_{ce} (electron gyrofrequency) [e.g., *Burtis and Helliwell*, 1969; *Meredith et al.*, 2001]. In contrast, plasmaspheric hiss is a relatively structureless broadband whistler mode emission generally observed inside the plasmasphere over a typical frequency range of 100–2000 Hz [*Thorne et al.*, 1973]. Both waves play important roles in the dynamical evolution of Earth's radiation belts [*Thorne*, 2010]. Chorus waves play a vital role in accelerating electrons to relativistic energies locally [*Horne et al.*, 2005; *Thorne et al.*, 2013; *Li et al.*, 2014] and can also precipitate ~10 keV electrons and thereby cause pulsating aurora [*Nishimura et al.*, 2010] and diffuse aurora [*Ni et al.*, 2008; *Thorne et al.*, 2010]. Plasmaspheric hiss is capable of precipitating more energetic electrons and therefore creating the slot region between the outer and inner radiation belts, which develops during relatively quiet periods after a geomagnetic storm [e.g., *Lyons and Thorne*, 1973; *Ni et al.*, 2013; *Breneman et al.*, 2015].

Magnetospheric chorus waves are typically generated by cyclotron resonant interactions with anisotropic superthermal electrons [*Kennel and Petschek*, 1966; *Li et al.*, 2009]. A portion of chorus emissions can propagate into the high-density plasmasphere via reflection at high latitudes and evolve into structureless hiss waves [*Bortnik et al.*, 2008, 2009; *Chen et al.*, 2009]. Pulsations in the Pc4-Pc5 band [*Li et al.*, 2011b] and density variations [*Li et al.*, 2011c] can modulate chorus excitation, while density variations also modulate hiss by local amplification and wave focusing mechanisms [*Moullard et al.*, 2002; *Chen et al.*, 2012a, 2012b].

In situ satellite measurements of whistler mode waves provide important wave properties, including the wave spectrum, polarization, and propagating direction [e.g., *Santolík et al.*, 2003a] from which we can

compile global statistical distributions over long periods of time. However, single satellite data can neither resolve whether wave modulations are due to spatial or temporal variation, nor determine the coherence scale of these wave structures. Besides, single satellite data cannot determine the cross L shell propagation of the waves and provide limited information about the spatial extent of the wave source region. In contrast, multiple satellites provide instantaneous multipoint wave observations, enabling us to distinguish between spatial and temporal variations, and also identify the wave coherence spatial scales. The terminology "coherence" in this paper refers to coherent modulation of an ensemble of wave spectra, but not wave phase, over a certain frequency range.

The spatial information of the waves is critical in linking the satellite observations, the ground-based aurora measurements, and the balloon observations, because the conjugated observations over time may differ by a distance up to several hours in magnetic local time (MLT) and several L shells. For example, *Breneman et al.* [2015] confirmed that the electron loss in the slot region arises from plasmaspheric hiss by correlating simultaneous observations from the Van Allen Probes and the Balloon Array for Radiation belt Relativistic Electron Losses, and in their case the two points differed by up to 3 h in MLT and 3 L shells. The pioneering study of the whistler mode wave coherence spatial scale can date back to the International Sun-Earth Explorer (ISEE) era as *Gurnett et al.* [1979] showed that the chorus wave coherent scale in the radiation belt region is less than the separation between two ISEE satellites, which is ~400 km. *Santolík and Gurnett* [2003] analyzed individual chorus elements measured by four Cluster satellites and obtained the typical chorus amplitude coherence scale of ~100 km at L = 4.4, which is about the wavelength. Using multisatellite measurement, *Agapitov et al.* [2010] obtained the chorus wave coherent scale of ~3000 km at L = 11, and most recently, *Němec et al.* [2016] obtained the quasiperiodic emissions coherent scale of ~1 R_E in the plasmasphere. The coherence scale of the electromagnetic ion cyclotron waves was also studied by correlating instantaneous measurements from two Van Allen Probes [*Blum et al.*, 2016].

Another implication of multipoint simultaneous measurements is tracing the wave propagation and locating the source. *Bortnik et al.* [2009] provided direct evidence that chorus waves are the source of hiss by presenting simultaneous observations from two of the Time History of Events and Macroscale Interactions during Substorms (THEMIS) satellites, and later *Li et al.* [2015] using coordinated observations of Van Allen Probe and THEMIS confirmed this scenario, and further demonstrated that chorus waves originated from a large L shell (~10), where it was previously considered unable to propagate into the plasmasphere, can in fact be the source of hiss.

In the present paper, we report coherent whistler mode waves over an unexpectedly large scale up to ~4.3 R_E, which were continuously observed by two Van Allen Probes over a period of 3.25 h. The cross correlations were calculated to investigate the time lag between the two-point observations and the frequency dependence. Finally, we discuss the possible source of these coherent whistler mode waves.

2. Observations

The twin Van Allen Probes traverse in roughly the same orbit (1.1 $R_E \times 5.8$ R_E, 10° inclination angle) with a varying separation that ranges from 0.1 to ~5 R_E [*Mauk et al.*, 2013]. On 5 November 2015 the apogee of the two Van Allen Probes was near the dayside (MLT = 14 h) and probe A lagged behind probe B by ~3.5 h. Figure 1a displays the orbits of the two probes over the time period of 05:25–08:40 UT, which occurred in the recovery phase of a geomagnetic storm indicated by the *SYM-H* index shown in Figure 1b. There were no significant substorm injections nor highly variable solar wind dynamic pressure during the 7 h preceding this time period, as shown by *AE* index in Figure 1c and by 1 min pressure data in Figure 1d, respectively.

Coherently modulated waves were clearly observed during 05:25–08:40 UT by the Electric and Magnetic Field Instrument Suite and Integrated Science (EMFISIS) Waves instrument [*Kletzing et al.*, 2013] on board the two probes which were separated by a distance of up to 4.3 R_E. Figures 2c and 2d show the wave magnetic spectra in a frequency range of 100–2000 Hz, and Figures 2e and 2f show the wave electric spectra in the spin plane (the spin axial wave component is not included due to instrumental spikes in the data). The ellipticity properties of these waves (Figures 2g and 2h) indicate that these coherent waves simultaneously observed by both probes were right-hand nearly circularly polarized whistler mode waves. In contrast to these whistler mode waves, magnetosonic waves, identified by their frequency range below the lower hybrid resonance

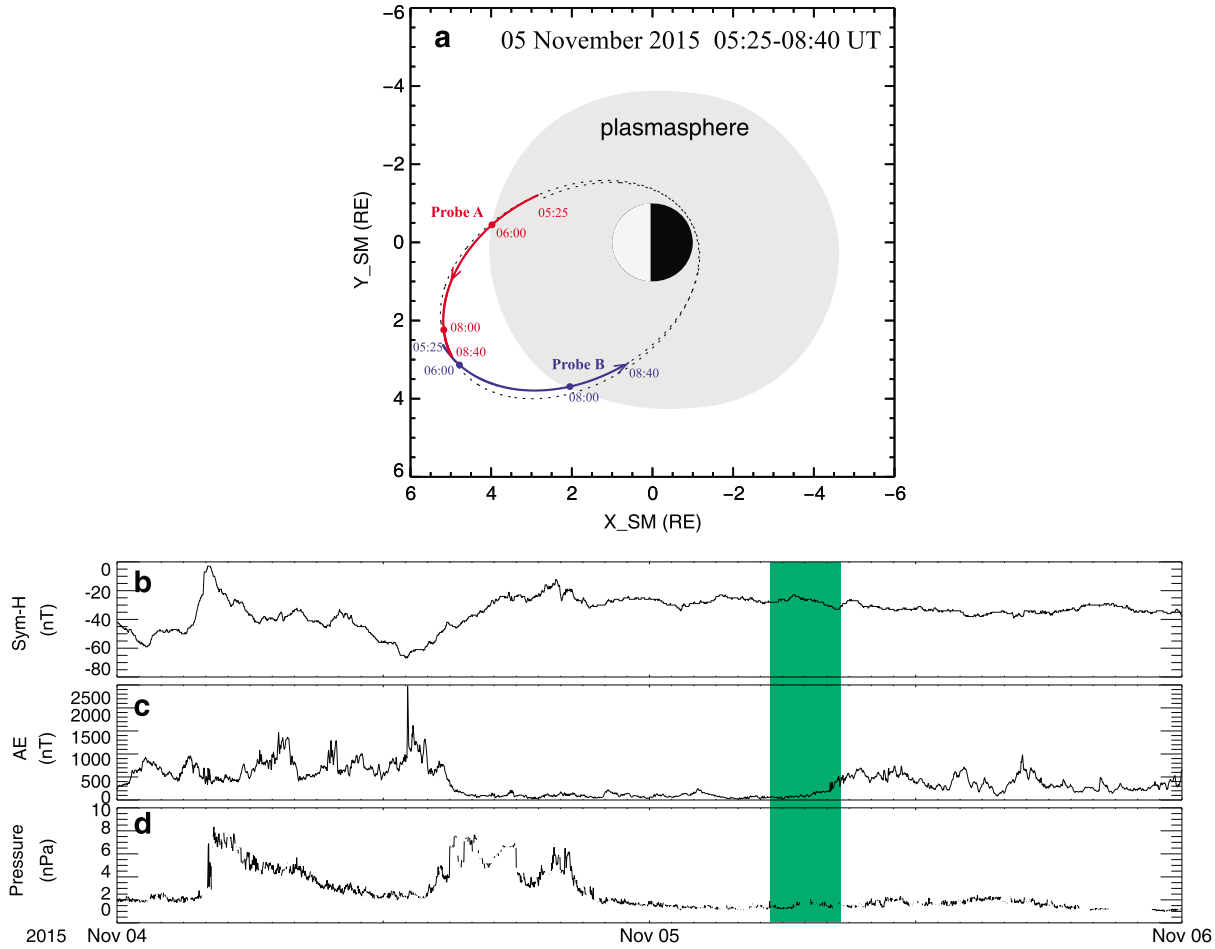

Figure 1. (a) The orbits of two Van Allen Probes with respect to a plasmapause modeled by a neural network [*Bortnik et al.*, 2016] and adjusted by in situ measurements. (b–d) The *AE* index, *SYM-H* index, and solar wind dynamic pressure from 04 November through 05 November 2015. The green area covers the period of wave observations shown in Figure 2.

frequency (f_{LHR}) and ellipticity close to 0 (i.e., linearly polarized), were observed by probe A during 05:50–06:20 UT, but they were not detected by probe B.

According to the satellite position with respect to the plasmapause, which was inferred from the upper hybrid frequency (f_{UHR}, a proxy of plasma density) measured by the High Frequency Receiver (HFR) as shown in Figures 2a and 2b, the observed period of wave coherence can be divided into three phases: (1) 05:25–06:00 UT, during which probe A was inside the plasmasphere while probe B was outside; (2) 06:00–08:00 UT, when both probes were outside the plasmasphere; and (3) 08:00–08:40 UT, when probe A was outside the plasmasphere but probe B traveled into the plasmasphere.

2.1. Plasmaspheric Hiss Associated With ULF Wave and Density Modulation

Figure 3a shows the plasma density inferred from the spacecraft potential [*Wygant et al.*, 2013] of probe A during the first coherent phase (probe A inside, probe B outside), and Figure 3b shows the magnetic field magnitude filtered between 20 s and 2 min. The density measurement fluctuates with the same period as the ~1 min ULF wave, and they were generally out of phase, possibly to maintain a quasi-equilibrium in the total pressure, except for a short period from 05:40 UT to 05:45 UT. Figure 3c displays the wave power spectral intensity measured by probe A. The wave amplitude peaks at magnetic field dips indicated by the dashed lines, suggesting that those hiss waves were possibly associated with Pc4-Pc5 ultralow frequency (ULF) waves. Figure 3e shows the wave power spectral intensity measured by probe B, and Figure 3d shows the integrated electric wave amplitudes measured by the two probes. The whistler mode waves observed by

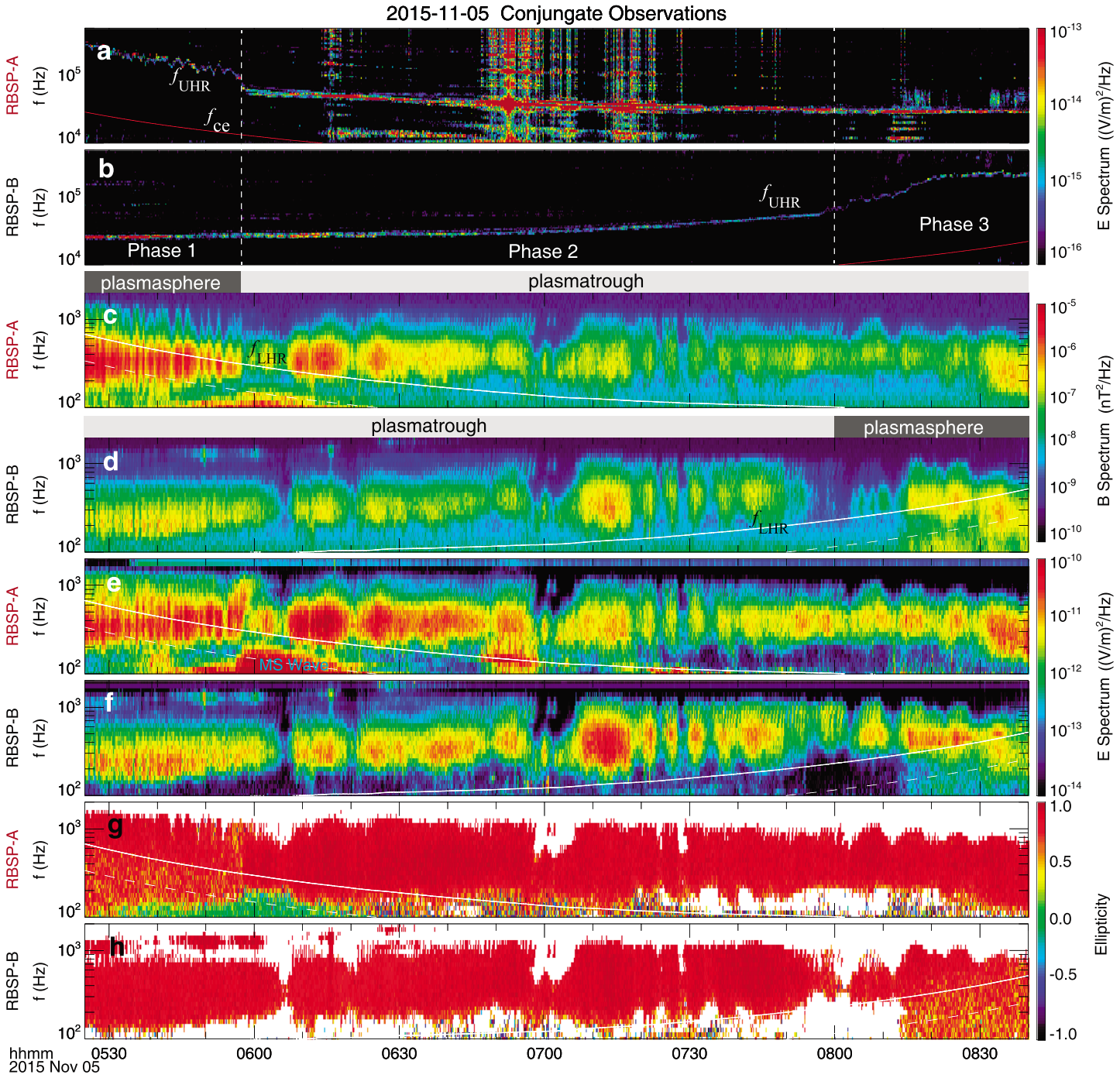

Figure 2. (a and b) The upper hybrid resonant frequency f_{UHR} measured by HFR onboard probes B and A, respectively, during 05:25–08:40 UT on 5 November 2015; (c and d) the 100–2000 Hz wave magnetic spectral intensities measured by WFR onboard the two probes; (e and f) the wave electric spectral intensities measured by the two probes; and (g and h) the wave ellipticity properties.

probe A and probe B show some correlation from 05:25 UT to 05:45 UT in the frequency range of 150–500 Hz, indicating that the hiss intensity variation is due to a temporal effect. The ULF wave measured by probe B (Figure 3f) also shows a good correlation with the whistler mode wave intensity. For a typical time period 05:35–05: 40 UT, the correlation between the 150–500 Hz wave amplitude and the ULF waves was 0.6 at probe A and 0.75 at probe B, as displayed in Figure 6d. The ULF waves measured by both probes (Figure 3f) show a good correlation during 05:25–05:45 UT, suggesting that the correlation of the whistler mode

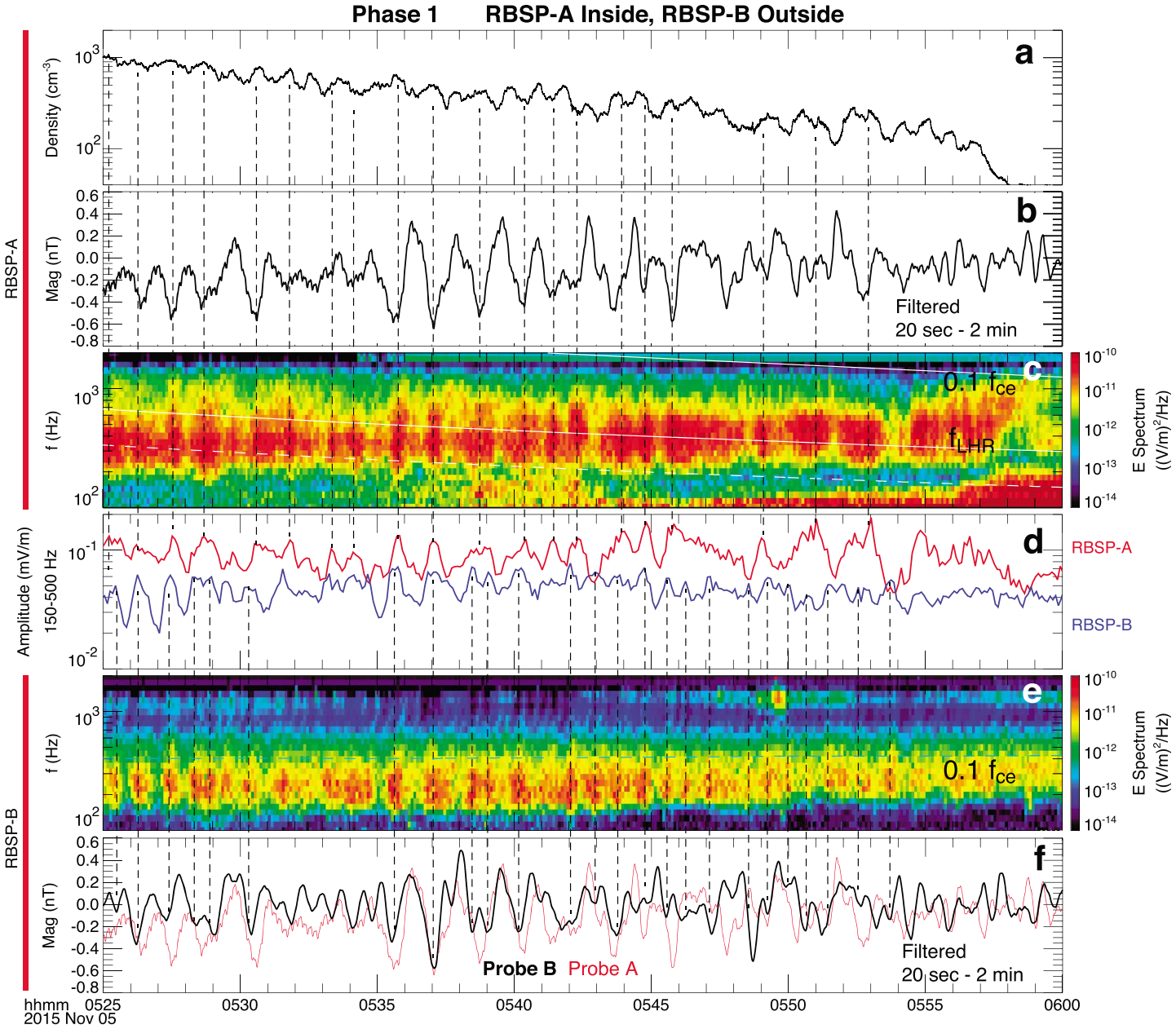

Figure 3. (a) The plasma density obtained from Van Allen Probe A spacecraft potential calibrated by f_{UHR}. (b) The magnetic field magnitude measured by probe A and filtered between 20 s and 2 min. (c) The wave magnetic spectrum in a frequency range of 100–2000 Hz measured by probe A. (d) The wave amplitude integrated from 150 Hz to 500 Hz measured by both probes, showing a correlation in the 150–500 Hz range during 05:25–05:45 UT. (e and f) The same as in Figures 3c and 3b but measured by probe B.

waves probably originated from the coherent ULF waves over a large spatial scale. The plasma density measured by probe B is not shown because the density calculated from the Van Allen Probe spacecraft potential has uncertainties in the low-density region ($<10\,\mathrm{cm}^{-3}$).

2.2. Periodic Rising-Tone Whistler Mode Waves

Figures 4a and 4b exhibit the zoomed in wave magnetic spectra measured by both probes during 06:40–07:40 UT, which is a period when both probes were outside the plasmapause. Periodic rising-tone emissions were observed by both probes over a frequency range of 500–1500 Hz, with a frequency sweep rate $\delta f/\delta t \simeq 700/1500$ Hz/min. Each element lasted for ~35–60 s, much longer than the ~0.1 s discrete chorus reported by *Santolík et al.* [2003b]. Such whistler mode periodic or quasiperiodic emissions with periods from 10 s to

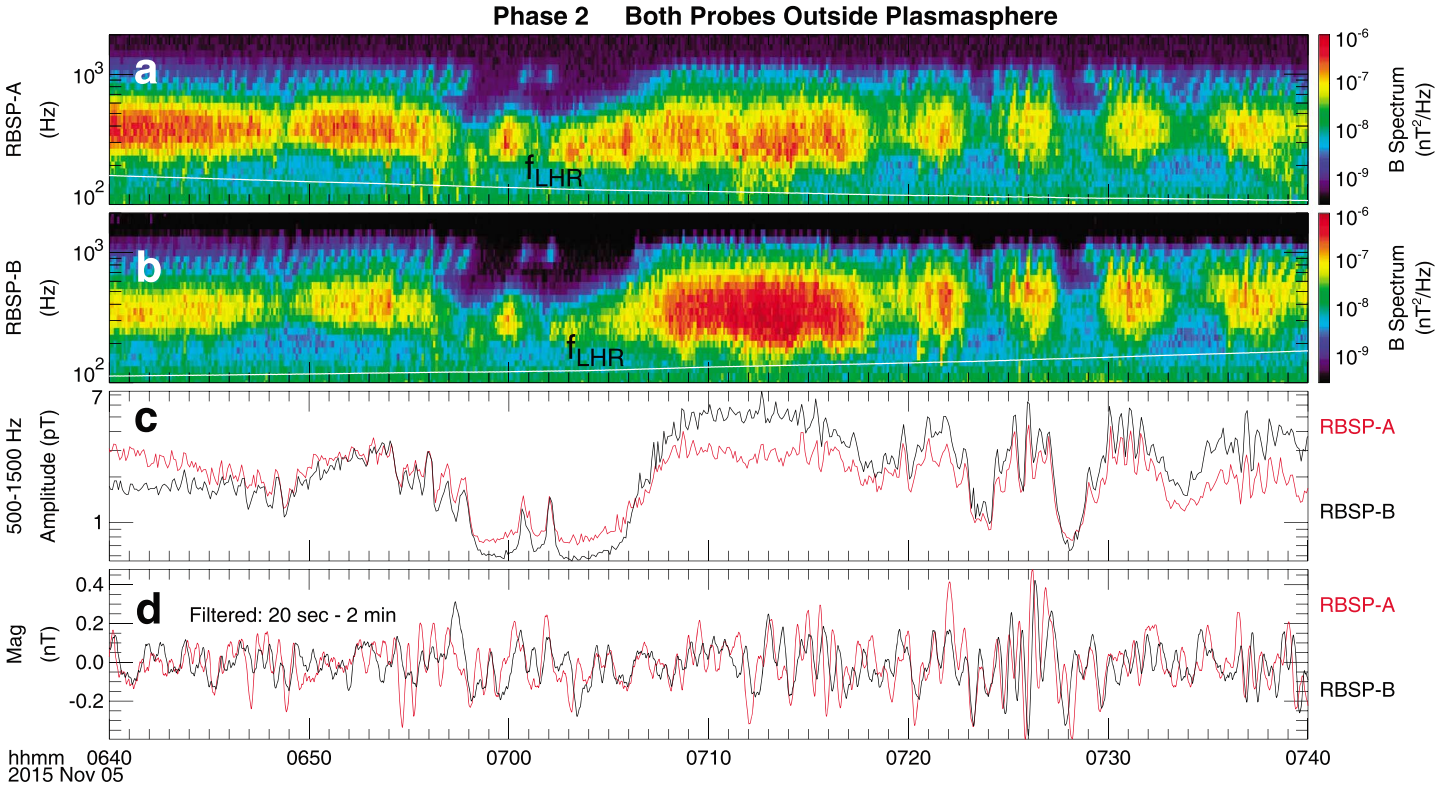

Figure 4. (a and b) The zoomed-in observations of wave electric spectrum by both probes respectively, during 06:40–07:40 UT, clearly showing the coherent periodic rising-tone emissions. (c) The wave amplitude integrated over 500–1500 Hz. (d) The magnetic field measured by both probes in the solar magnetic coordinate system and filtered between 20 and 120 s.

several minutes have been reported by ground observations [e.g., *Carson et al.*, 1965; *Smith et al.*, 1998; *Manninen et al.*, 2014] and satellite observations [e.g., *Hayosh et al.*, 2014; *Němec et al.*, 2013, 2014, 2016]. These periodic rising-tone emissions, as well as the 150–500 Hz lower frequency waves, were strongly coherent at the position of the two probes, even though they were separated with a spatial distance up to 4.3 R_E and a MLT difference up to ~3 h. The coherence spatial scale of these waves is much larger than that of typical discrete chorus (~100 km) [*Santolík and Gurnett*, 2003] in the radiation belt.

Figure 4c displays the wave amplitudes integrated over 500–1500 Hz during Phase 2, and Figure 4d displays the magnetic field magnitudes filtered between 20 s and 2 min. Although the magnetic field shows a fluctuation with approximately the same period as those rising-tone emissions, there was no obvious one-to-one correspondence between the periodic rising-tone emissions and the ULF fluctuations. This is consistent with the Cluster event study of the quasiperiodic emissions and the ULF waves [*Němec et al.*, 2013]. For a typical time period 07:15–07:20 UT, the correlation between the two is small (<0.4) at the locations of both probes, as shown in Figure 6e. The whistler mode waves were very well correlated at the locations of the two satellites during the entire Phase 2, but the ULF waves measured by the two probes were not persistently coherent over a periodicity range of 20–120 s. One potential explanation of this observation is that the ~1 min periodic emission, as well as the overall modulation of these whistler mode waves, may have originated from a common source located at high L shells, where the periodic rising-tone emissions were locally modulated by the ULF waves.

During the third phase when probe B traveled into the plasmapause, the >500 Hz periodic whistler mode waves, as well as the <500 Hz waves which have larger intensities and vary over longer periods, were still coherent at the locations of the two probes, as shown in Figures 5a and 5b. Again, the recurring period of the whistler mode waves and the period of the ULF waves were close, but there was no one-to-one correlation between the wave amplitudes (Figure 5c) and the ULF fluctuations (Figure 5d). The correlation between the two is small at the locations of both probes, as displayed in Figure 6f. In the course of the 2 h and 40 min of coherent observations during the entire second and third phases, the two spacecraft both changed their L

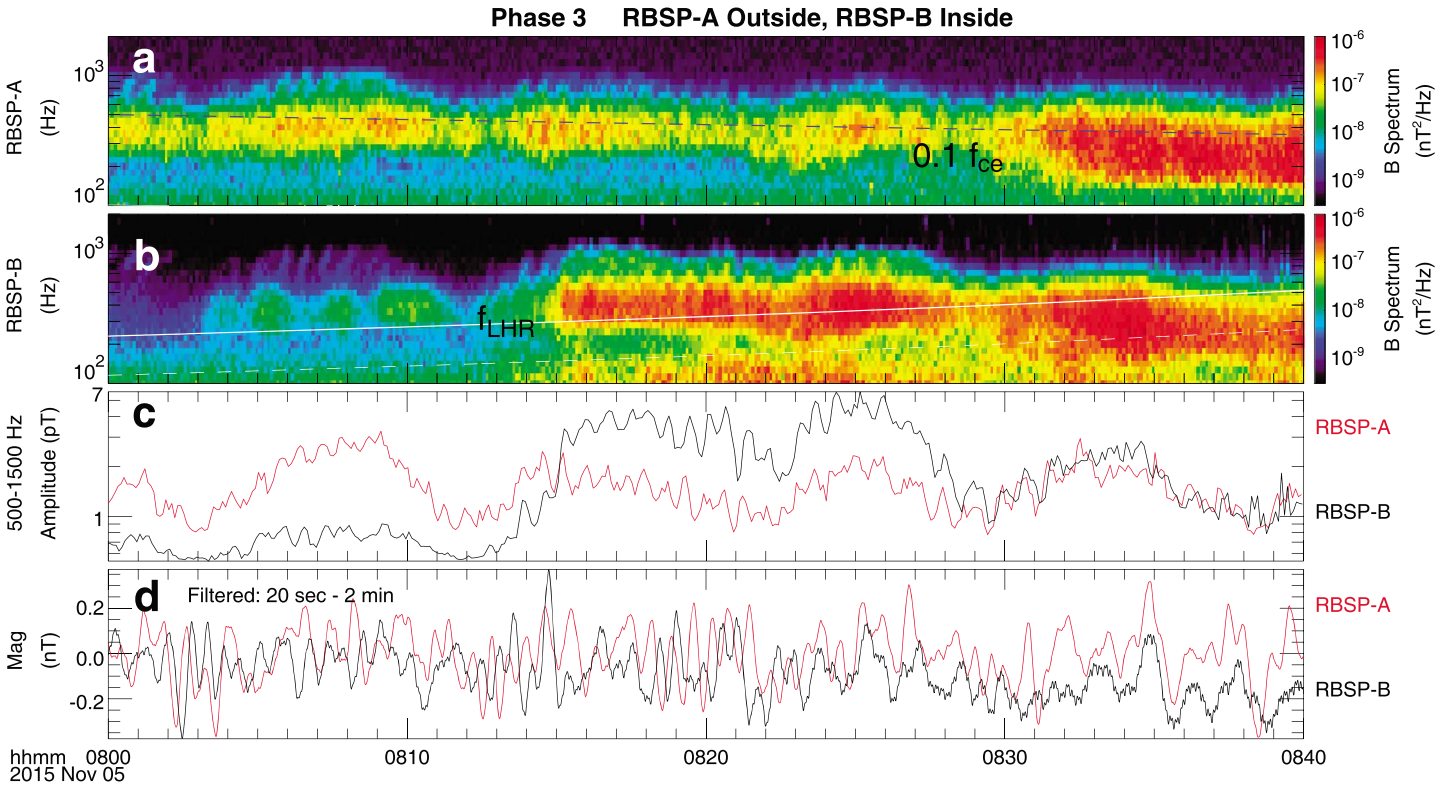

Figure 5. The same as Figure 4 but for the third phase during 08:00–08:40 UT.

shells and MLTs in the course of their respective orbits, and even switched their relative separation in L shell, as shown in Figure 1a (i.e., at ~06:00 UT A was the inner probe and B was the outer probe, whereas at ~08:00 UT A advanced to its apogee and became the outer probe whereas B became the inner probe). Regardless of the relative configuration of the spacecraft, they continue to observe coherent modulation of the waves on both spacecraft, suggesting that the entire postnoon region over L~3.4–5.8 was filled with coherently modulated whistler mode waves.

3. Implications Concerning the Wave Source

During the first coherent phase, a good correlation was observed between the whistler mode waves in the plasmatrough and the hiss waves in the plasmasphere. A careful examination of the wave amplitudes in Figure 3d indicates that the waves occurred at probe B (outer probe) a few seconds earlier than at probe A (inner probe). In order to show the correlation at each frequency, a cross-correlation analysis is performed between probe A and probe B wave observations as a function of frequency and time lag. The cross correlation at a representative time of 05:35 UT in Figure 6a shows that the 150–500 Hz waves detected by probe B were observed ~6 s earlier than that by probe A (the positive lag indicates that probe B measurements come later than probe A), while the higher-frequency waves exhibited little correlation. Note that the time resolution of the wave spectrum in survey mode is 6 s, and we linearly interpolated the wave data into 1 s resolution. Therefore, the fact that probe B observed the waves prior to probe A is unchanged, but the ~6 s delay may not be accurate. The coincident ULF wave observations with 1 s cadence indicate that probe B observed the ULF waves earlier than probe A by a few seconds (Figure 3f), and a cross correlation between the compressional ULF fluctuations measured by the two probes during 05:25–05:45 UT reveals that the time difference of the ULF waves was ~5 s (not shown), which is roughly consistent with the time lag of the 150–500 Hz whistler mode waves measured by the two probes.

The whistler mode chorus waves can be modulated by large-amplitude compressional ULF pulsations, which significantly change the electron resonant energy and thus the number of resonant electrons, or significantly change the electron anisotropy [*Li et al.*, 2011b]. The plasmaspheric hiss can be modulated by plasma density

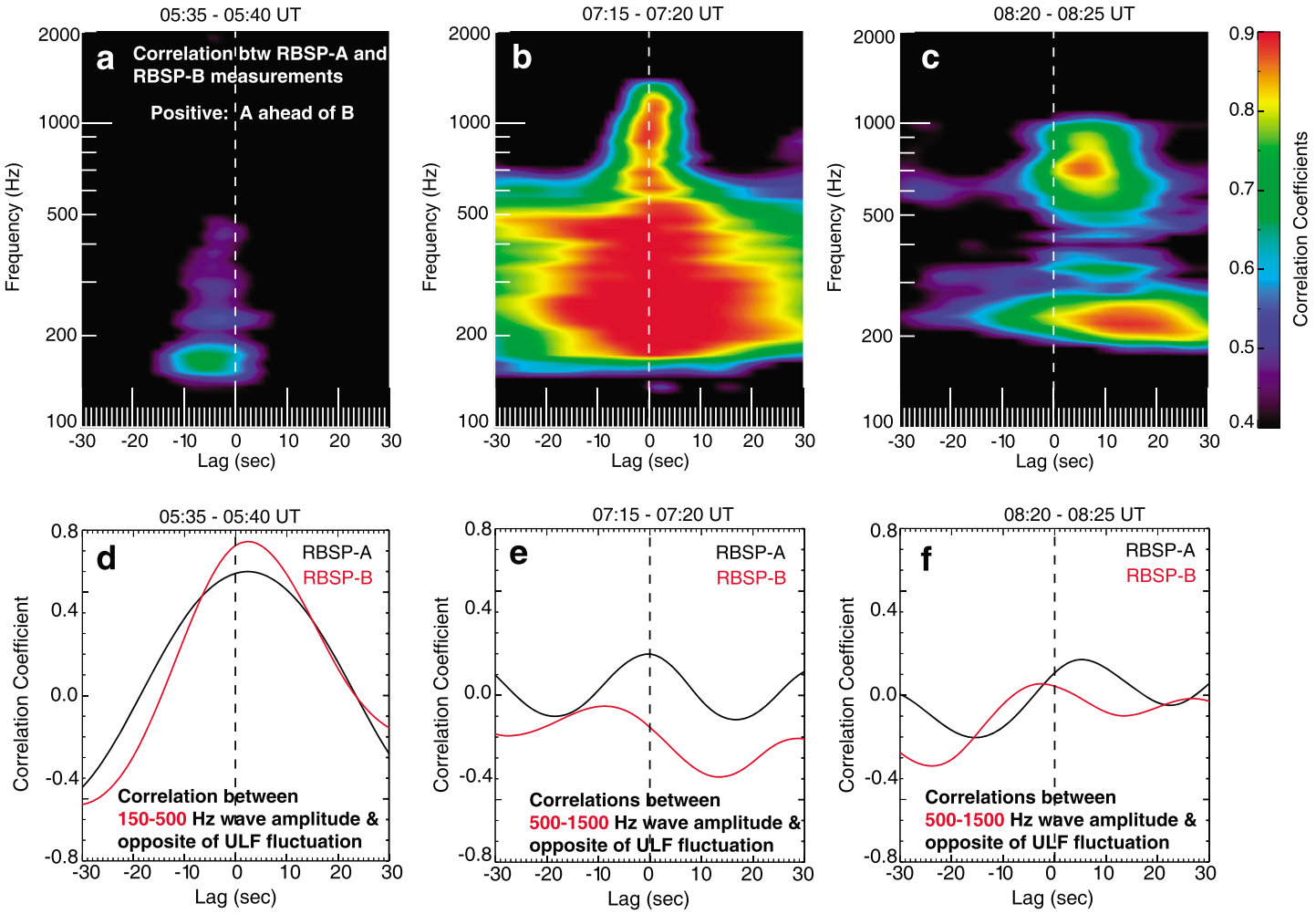

Figure 6. (a–c) The cross-correlation coefficients of coherent waves between two probe measurements at three representative time periods, each represents one coherent phase. Positive time lag indicates that probe B observations lag behind probe A. (d–f) The cross-correlation coefficients between the whistler mode wave amplitude and the ULF fluctuation at both probes during those three periods. We used the opposite value of ULF magnitude in the cross-correlation calculations because the ULF magnitudes were anticorrelated with whistler mode waves during Phase 1.

via two mechanisms, local amplification via an instability [*Chen et al.*, 2012b], and ray focusing effect at density crests [*Chen et al.*, 2012a, 2012b]. The relative magnetic fluctuations ($\delta B/B_0$) observed by both probes during the first coherent phase were about 0.1%–0.2%, and thus are not capable of significantly modulating the electron resonant energy. The density fluctuation in this event exhibited a temporal variation because it was correlated with the ULF waves which were coherent over a large spatial scale, and the density possibly varies simultaneously on a large spatial scale.

During Phase 1, The whistler mode wave intensity measured inside the plasmasphere by Probe A is significantly larger than that measured outside by Probe B. We further investigate the possible excitation mechanism of whistler mode waves by analyzing both wave and electron data. Figures 7a–7c show the plasma density, wave spectra, and wave normal angles, respectively, measured by probe A over the entire coherent period. Figures 7d and 7e show the electron anisotropy calculated following *Chen et al.* [1999], and flux over an energy range of 30–4000 keV measured by the Magnetic Electron Ion Spectrometer (MagEIS) instrument [*Blake et al.*, 2013] along probe A orbit. The same measurements by Probe B are shown in Figures 7f–7j. The cyclotron resonant energy for plasmaspheric hiss observed by Probe A during Phase 1 was $>\sim$100 keV (e.g., for the 350 Hz waves with a wave normal angle 30°, the resonant energy at L = 3.2 with a background density 800 cm^{-3} is 200 keV, and that at L = 3.8 with a background density 300 cm^{-3} is 115 keV). We see that the electrons exhibited a high anisotropy inside the plasmasphere, which can potentially lead to local amplification of the hiss waves [*Chen et al.*, 2012b]. These hiss waves were likely to be modulated by the density

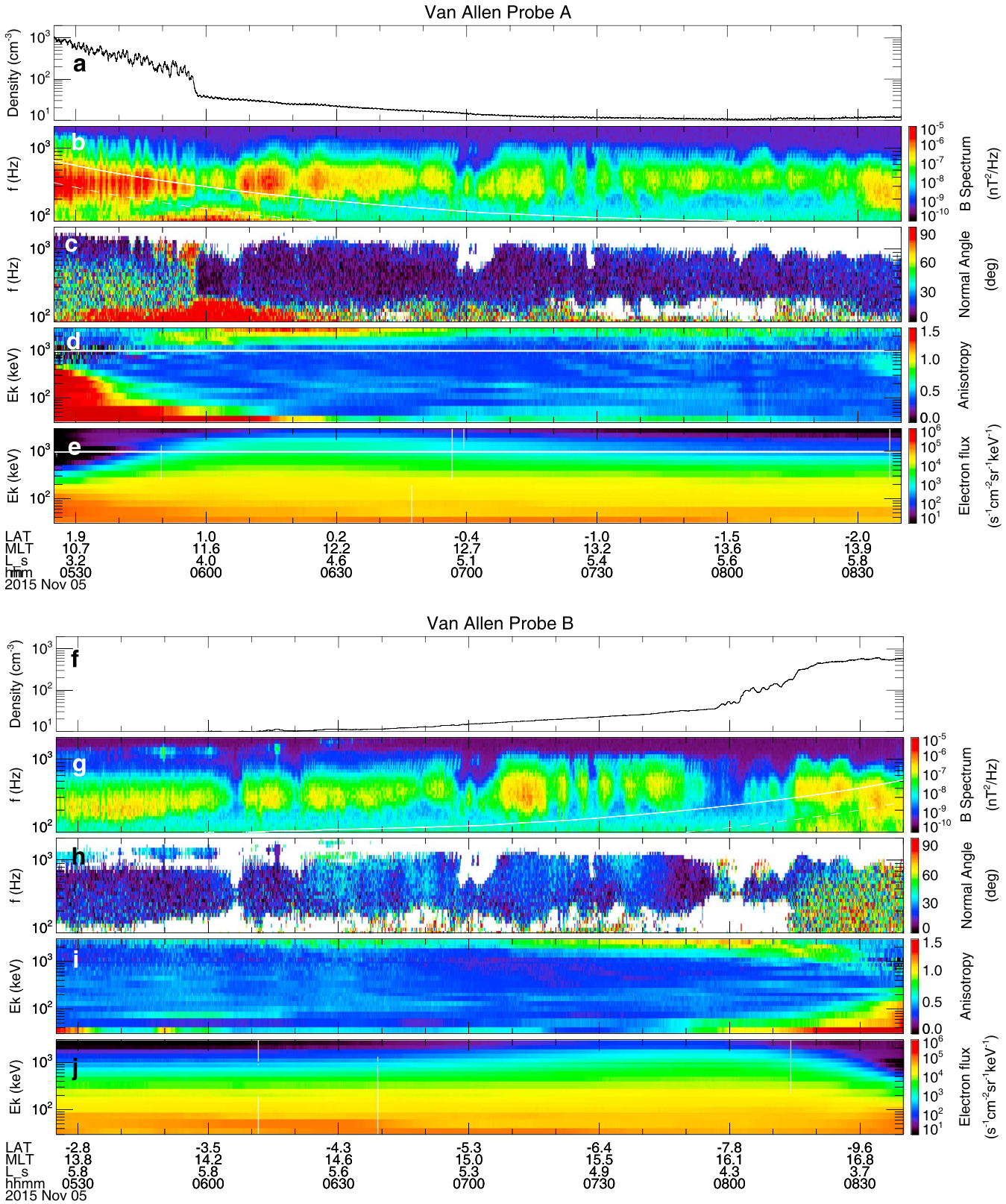

Figure 7. (a) The density inferred from the spacecraft potential measured by probe A during the entire coherent period. (b) The wave magnetic spectral intensities and (c) the wave normal angles measured over the same period. (d) The electron anisotropy and (e) the electron flux measured by the MagEIS instrument onboard probe A in an energy range of 30–4000 keV. (f–j) The same as in Figures 7a–7e but measured by probe B during the same period.

because the high density lowers the resonant energy and hence increases the number of resonant electrons. In contrast, the emissions observed by probe B in the plasmatrough region were unlikely locally amplified, because the minimum resonant energy for 300 Hz waves with a 0° normal angle at L = 5.8 and an estimated density of 5 cm^{-3} is 130 keV; however, the electron anisotropy was not high at energies above 90 keV. Calculations of wave growth rates are needed to determine if those hiss waves are locally excited, and the proposed idea that ULF wave drives density variation and modulates the whistler mode wave intensity needs to be tested by other multipoint observations and ray tracing simulations [*Horne*, 1989] in the future.

Figure 6b displays the cross correlation at 07:15 UT, which is a representative time for the second coherent phase when both probes were outside the plasmasphere. It is evident that the waves observed by the two probes were well correlated in the frequency range of 150–1500 Hz, and no clear time lag is seen between these two probes. The time lag range of good correlations is significantly narrower for higher-frequency waves (500–1500 Hz), because their typical time scale (~35–60 s) is shorter than that of the modulation over 150–500 Hz (~2–10 min). These 500–1500 Hz periodic rising-tone emissions can resonate with $>$ ~20 keV electrons, but the electron flux above 32 keV measured by the MagEIS with a cadence of 11 s did not exhibit an ~35–60 s periodic structure and the anisotropy was not high. The electrons at lower energies measured by the Helium Oxygen Proton Electron (HOPE) [*Funsten et al.*, 2013] instrument did not show a periodic modulation either, and the anisotropy was low (not shown). Since the whistler mode wave modulation was coherent over a large spatial scale and across several L shells, we suggest that they probably originated from one single source and are not locally generated. The ray tracing simulations [*Bortnik et al.*, 2008] suggest that although the whistler mode waves propagate in quasi-parallel direction to the ambient magnetic field at the origin, they can be very oblique at higher latitudes and can be reflected back into the low latitudes at lower L shells, and in this process the waves are scattered to a wide L shell and MLT ranges. The typical propagation time is a few seconds [*Bortnik et al.*, 2008], which is significantly shorter than the recurring period, and hence, the coherent waves were observed almost simultaneously at the two probes.

For the third coherent phase, the cross correlation indicates an evident positive time lag (Figure 6c), which means that probe A (outer) observed the waves ~6 s earlier than probe B (inner). This supports the scenario that these whistler mode waves originate in the plasmatrough and propagate into the plasmasphere [*Bortnik et al.*, 2008, 2011; *Chen et al.*, 2009]. The inner probe observed the periodic emissions later probably due to a longer propagation path. Note that the whistler mode waves propagate slower in the high-density plasmasphere. The refractive index of the right-hand polarized whistler mode waves can be approximated as $n^2 = \omega_{pe}^2/\omega(\omega_{ce} - \omega)$, where $\omega_{pe} = \sqrt{ne^2/\epsilon_0 m_e}$ represents the electron plasma frequency which is proportional to square root of plasma density n, ω is the wave frequency, and ω_{ce} is the unsigned electron cyclotron frequency. We find that the phase velocity, c/n, decreases as plasma density increases. Assuming that these waves were originally in the typical chorus frequency range of ~0.1–0.5 f_{ce} at the excitation region, the most probable source region of these waves was L = 7.0–8.3 near the dayside, but the detailed excitation mechanism of these periodic emissions remains as an outstanding question.

During the whole coherent period, the THEMIS-A, D, and E satellites [*Angelopoulos*, 2008] were in the postmidnight sector, the Cluster constellation was in the premidnight sector, and none of them observed whistler mode waves. The Magnetospheric Multiscale [*Burch et al.*, 2016] satellites were on the postnoon side which was at the same MLT as the Van Allen Probe apogee; however, they were in the magnetosheath region (~10 R_E) and measured locally generated discrete whistler mode waves that were below ~300 Hz and not correlated with the Van Allen Probe observations. Observations from these multiple satellites indicate that the whistler mode waves observed by Van Allen probes, although were coherent over a large spatial scale, were not present across the entire magnetosphere.

4. Conclusions

Coherent whistler mode waves were observed both inside and outside the plasmapause for over 3.25 h on 5 November 2015 by two Van Allen Probes with a large separation up to 4.3 R_E. The coherence existed when the two probes traversed across various MLTs and L shells. At different stages of spacecraft spatial configuration, the coherence exhibited different characteristics and showed a frequency dependence. During the first coherent phase (the two probes were separated by the plasmapause), the 150–500 Hz whistler mode waves

observed in the plasmatrough were well correlated with the density-modulated plasmaspheric hiss which had a stronger intensity and a wider frequency range (150–1500 Hz). The plasmaspheric hiss was probably amplified by the local anisotropic electrons and was modulated by density which modulated the number of resonant electrons. The plasmaspheric density modulation was correlated to a large-scale coherent ULF wave, and therefore was probably a temporal variation rather than a spatial variation. During the second phase (both probes were outside the plasmapause) and the third phase (the leading probe traveled into the plasmasphere, and the trailing probe moved outside of the plasmasphere), the 500–1500 Hz rising-tone emissions with ~35–60 s separation were coherent over an unexpectedly large spatial scale and even across the plasmapause. The cross correlation between two probe conjugate measurements during the third phase suggests that the 500–1500 periodic rising-tone emissions were probably propagated in from higher L shells.

The discovery that the amplitude coherent scale of whistler mode waves can be up to 4.3 R_E approves the validity of linking the observations from the satellites, the ground-based All-Sky Imagers, and the balloons that have certain spatial separations in their footprints. The coherence scale in this study is significantly larger than that of the discrete rising-tone chorus waves reported in a wide radial range from L = 4.4 to L = 11 [*Gurnett et al*., 1979; *Santolík and Gurnett*, 2003; *Agapitov et al*., 2010]. This is possibly because the rising-tone chorus waves in the previously reported cases were measured at the excitation region and the coherence scale is small, while the coherent waves in this study are due to propagations across the field lines. With these multipoint observations together with ray tracing technique [*Horne*, 1989], we will be capable of better understanding the propagation of the waves and their origin, which is beyond the scope of the present paper and is left for future investigations.

Acknowledgments

J.L. and J.B. would like to acknowledge the NASA grant NNX13AI61G. We also thank EMFISIS subaward 1001057397:01; the ECT subaward 13-041; NSF Geospace Environment Modeling grant AGS-1723342, and NASA grants NNX14AN85G, NNX11AR64G, NNX17AD15G, and NNX15AI96G. This work was also supported by JHU/APL contracts 967399 and 921647 under NASA's prime contract NAS5-01072. We acknowledge the Van Allen Probes data from the EMFISIS instrument obtained from https://emfisis.physics.uiowa.edu/data/index, the EFW instrument data obtained from http://www.space.umn.edu/missions/rbspefw-home-university-of-minnesota/, and the MagEIS and HOPE data were downloaded from Van Allen Probe ECT website at http://www.rbsp-ect.lanl.gov/. We also thank the World Data Center for Geomagnetism, Kyoto, for providing *SYM-H* and *AE* indexes (http://wdc.kugi.kyoto-u.ac.jp/aeasy/index.html), and the Space Physics Data Facility at the NASA Goddard Space Flight Center for providing the OMNI2 data (ftp://spdf.gsfc.nasa.gov/pub/data/omni/omni_cdaweb/).

References

Agapitov, O., V. Krasnoselskikh, Y. Zaliznyak, V. Angelopoulos, O. LeContel, and G. Rolland (2010), Chorus source region localization in the Earth's outer magnetosphere using THEMIS measurements, *Ann. Geophys.*, *28*, 1377–1386, doi:10.5194/angeo-28-1377-2010.

Angelopoulos, V. (2008), The THEMIS mission, *Space Sci. Rev.*, *141*(1–4), 5–34, doi:10.1007/s11214-008-9336-1.

Blake, J., et al. (2013), The magnetic electron ion spectrometer (mageis) instruments aboard the radiation belt storm probes (rbsp) spacecraft, *Space Sci. Rev.*, *179*, 383–421, doi:10.1007/s11214-013-9991-8.

Blum, L. W., O. Agapitov, J. W. Bonnell, C. Kletzing, and J. Wygant (2016), EMIC wave spatial and coherence scales as determined from multipoint Van Allen Probe measurements, *Geophys. Res. Lett.*, *43*, 4799–4807, doi:10.1002/2016GL068799.

Bortnik, J., R. M. Thorne, and N. P. Meredith (2008), The unexpected origin of plasmaspheric hiss from discrete chorus emissions, *Nature*, *452*, 62–66, doi:10.1038/nature06741.

Bortnik, J., W. Li, R. M. Thorne, V. Angelopoulos, C. Cully, J. Bonnell, O. Le Contel, and A. Roux (2009), An observation linking the origin of plasmaspheric hiss to discrete chorus emissions, *Science*, *324*, 775, doi:10.1126/science.1171273.

Bortnik, J., L. Chen, W. Li, R. M. Thorne, N. P. Meredith, and R. B. Horne (2011), Modeling the wave power distribution and characteristics of plasmaspheric hiss, *J. Geophys. Res.*, *116*, A12209, doi:10.1029/2011JA016862.

Bortnik, J., W. Li, R. M. Thorne, and V. Angelopoulos (2016), A unified approach to inner magnetospheric state prediction, *J. Geophys. Res. Space Physics*, *121*, 2423–2430, doi:10.1002/2015JA021733.

Breneman, A. W., et al. (2015), Global-scale coherence modulation of radiation-belt electron loss from plasmasphric hiss, *Nature*, *523*, 193–195, doi:10.1038/nature14515.

Burch, J. L., T. E. Moore, R. B. Torbert, and B. L. Giles (2016), Magnetospheric multiscale overview and science objectives, *Space Sci. Rev.*, *199*, 5–21, doi:10.1007/s11214-015-0164-9.

Burtis, W. J., and R. A. Helliwell (1969), Banded chorus—A new type of VLF radiation observed in the magnetosphere by OGO 1 and OGO 3, *J. Geophys. Res.*, *74*(11), 3002–3010, doi:10.1029/JA074i011p03002.

Carson, W. B., J. A. Koch, J. H. Pope, and R. M. Gallet (1965), Long-period very low frequency emission pulsations, *J. Geophys. Res.*, *70*(17), 4293–4303, doi:10.1029/JZ070i017p04293.

Chen, L., J. Bortnik, R. M. Thorne, R. B. Horne, and V. K. Jordanova (2009), Three-dimensional ray tracing of VLF waves in a magnetospheric environment containing a plasmaspheric plume, *Geophys. Res. Lett.*, *36*, L22101, doi:10.1029/2009GL040451.

Chen, L., J. Bortnik, W. Li, R. M. Thorne, and R. B. Horne (2012a), Modeling the properties of plasmaspheric hiss: 2. Dependence on the plasma density distribution, *J. Geophys. Res.*, *117*, A05202, doi:10.1029/2011JA017202.

Chen, L., R. M. Thorne, W. Li, J. Bortnik, D. Turner, and V. Angelopoulos (2012b), Modulation of plasmaspheric hiss intensity by thermal plasma density structure, *Geophys. Res. Lett.*, *39*, L14103, doi:10.1029/2012GL052308.

Chen, M. W., J. L. Roeder, J. F. Fennell, L. R. Lyons, R. L. Lambour, and M. Schulz (1999), Proton ring current pitch angle distributions: Comparison of simulations with CRRES observations, *J. Geophys. Res.*, *104*, 17,379–17,389, doi:10.1029/1999JA900142.

Funsten, H. O., et al. (2013), Helium, Oxygen, Proton, and Electron (HOPE) mass spectrometer for the Radiation Belt Storm Probes mission, *Space Sci. Rev.*, *179*, 423–484, doi:10.1007/s11214-013-9968-7.

Gurnett, D. A., R. R. Anderson, F. L. Scarf, R. W. Fredricks, and E. J. Smith (1979), Initial results from the ISEE 1 and 2 plasma wave investigation, *Space Sci. Rev.*, *23*, 103–122.

Hayosh, M., F. Němec, O. Santolík, and M. Parrot (2014), Statistical investigation of VLF quasiperiodic emissions measured by the DEMETER spacecraft, *J. Geophys. Res. Space Physics*, *119*, 8063–8072, doi:10.1002/2013JA019731.

Horne, R. B. (1989), Path-integrated growth of electrostatic waves: The generation of terrestrial myriametric radiation, *J. Geophys. Res.*, *94*, 8895–8909, doi:10.1029/JA094iA07p08895.

Horne, R. B., et al. (2005), Wave acceleration of electrons in the Van Allen radiation belts, *Nature*, *437*, 227–230, doi:10.1038/nature03939.

Kennel, C. F., and H. E. Petschek (1966), Limit on stable trapped particle fluxes, *J. Geophys. Res.*, *71*, 1–28, doi:10.1029/JZ071i001p00001.

Kletzing, C., et al. (2013), The Electric and Magnetic Field Instrument Suite and Integrated Science (EMFISIS) on RBSP, *Space Sci. Rev.*, *179*, 127–181, doi:10.1007/s11214-013-9993-6.

Li, W., R. M. Thorne, V. Angelopoulos, J. W. Bonnell, J. P. McFadden, C. W. Carlson, O. LeContel, A. Roux, K. H. Glassmeier, and H. U. Auster (2009), Evaluation of whistler-mode chorus intensification on the nightside during an injection event observed on the THEMIS spacecraft, *J. Geophys. Res.*, *114*, A00C14, doi:10.1029/2008JA013554.

Li, W., J. Bortnik, R. M. Thorne, and V. Angelopoulos (2011a), Global distribution of wave amplitudes and wave normal angles of chorus waves using THEMIS wave observations, *J. Geophys. Res.*, *116*, A12205, doi:10.1029/2011JA017035.

Li, W., R. M. Thorne, J. Bortnik, Y. Nishimura, and V. Angelopoulos (2011b), Modulation of whistler mode chorus waves: 1. Role of compressional Pc4–5 pulsations, *J. Geophys. Res.*, *116*, A06205, doi:10.1029/2010JA016312.

Li, W., J. Bortnik, R. M. Thorne, Y. Nishimura, V. Angelopoulos, and L. Chen (2011c), Modulation of whistler mode chorus waves: 2. Role of density variations, *J. Geophys. Res.*, *116*, A06206, doi:10.1029/2010JA016313.

Li, W., et al. (2014), Radiation belt electron acceleration by chorus waves during the 17 March 2013 storm, *J. Geophys. Res. Space Physics*, *119*, 4681–4693, doi:10.1002/2014JA019945.

Li, W., L. Chen, J. Bortnik, R. M. Thorne, V. Angelopoulos, C. A. Kletzing, W. S. Kurth, and G. B. Hospodarsky (2015), First evidence for chorus at a large geocentric distance as a source of plasmaspheric hiss: Coordinated THEMIS and Van Allen Probes observation, *Geophys. Res. Lett.*, *42*, 241–248, doi:10.1002/2014GL062832.

Lyons, L. R., and R. M. Thorne (1973), Equilibrium structure of radiation belt electrons, *J. Geophys. Res.*, *78*(13), 2142–2149, doi:10.1029/JA078i013p02142.

Manninen, J., A. G. Demekhov, E. E. Titova, A. E. Kozlovsky, and D. L. Pasmanik (2014), Quasiperiodic VLF emissions with short-period modulation and their relationship to whistlers: A case study, *J. Geophys. Res. Space Physics*, *119*, 3544–3557, doi:10.1002/2013JA019743.

Mauk, B. H., N. J. Fox, S. G. Kanekal, R. L. Kessel, D. G. Sibeck, and A. Ukhorskiy (2013), Science objectives and rationale for the radiation belt storm probes mission, *Space Sci. Rev.*, *179*, 3–27, doi:10.1007/s11214-012-9908-y.

Meredith, N. P., R. B. Horne, and R. R. Anderson (2001), Substorm dependence of chorus amplitudes: Implications for the acceleration of electrons to relativistic energies, *J. Geophys. Res.*, *106*(A7), 13,165–13,178, doi:10.1029/2000JA900156.

Moullard, O., A. Masson, H. Laakso, M. Parrot, P. Decreau, O. Santolik, and M. Andre (2002), Density modulated whistler mode emissions observed near the plasmapause, *Geophys. Res. Lett.*, *29*(20), 1975, doi:10.1029/2002GL015101.

Němec, F., et al. (2013), Quasiperiodic emissions observed by the Cluster spacecraft and their association with ULF magnetic pulsations, *J. Geophys. Res. Space Physics*, *118*, 4210–4220, doi:10.1002/jgra.50406.

Němec, F., J. S. Pickett, and O. Santolík (2014), Multispacecraft Cluster observations of quasiperiodic emissions close to the geomagnetic equator, *J. Geophys. Res. Space Physics*, *119*, 9101–9112, doi:10.1002/2014JA020321.

Němec, F., G. Hospodarsky, J. S. Pickett, O. Santolík, W. S. Kurth, and C. Kletzing (2016), Conjugate observations of quasiperiodic emissions by the Cluster, Van Allen Probes, and THEMIS spacecraft, *J. Geophys. Res. Space Physics*, *121*, 7647–7663, doi:10.1002/2016JA022774.

Ni, B., R. M. Thorne, Y. Y. Shprits, and J. Bortnik (2008), Resonant scattering of plasma sheet electrons by whistler-mode chorus: Contribution to diffuse aurora precipitation, *Geophys. Res. Lett.*, *35*, L11106, doi:10.1029/2008GL034032.

Ni, B., J. Bortnik, R. M. Thorne, Q. Ma, and L. Chen (2013), Resonant scattering and resultant pitch angle evolution of relativistic electrons by plasmaspheric hiss, *J. Geophys. Res. Space Physics*, *118*, 7740–7751, doi:10.1002/2013JA019260.

Nishimura, Y., et al. (2010), Identifying the driver of pulsating aurora, *Science*, *330*, 81–84, doi:10.1126/science.1193186.

Santolík, O., and D. A. Gurnett (2003), Transverse dimensions of chorus in the source region, *Geophys. Res. Lett. 30*(2), 1031, doi:10.1029/2002GL016178.

Santolík, O., M. Parrot, and F. Lefeuvre (2003a), Singular value decomposition methods for wave propagation analysis, *Radio Sci.*, *38*(1), 1010, doi:10.1029/2000RS002523.

Santolík, O., D. A. Gurnett, J. S. Pickett, M. Parrot, and N. Cornilleau-Wehrlin (2003b), Spatio-temporal structure of storm-time chorus, *J. Geophys. Res.*, *108*(A7), 1278, doi:10.1029/2002JA009791.

Smith, A. J., M. J. Engebretson, E. M. Klatt, U. S. Inan, R. L. Arnoldy, and H. Fukunishi (1998), Periodic and quasiperiodic ELF/VLF emissions observed by an array of Antarctic stations, *J. Geophys. Res.*, *103*(A10), 23,611–23,622, doi:10.1029/98JA01955.

Thorne, R. M. (2010), Radiation belt dynamics: The importance of wave-particle interactions, *Geophys. Res. Lett.*, *37*, L22107, doi:10.1029/2010GL044990.

Thorne, R. M., E. J. Smith, R. K. Burton, and R. E. Holzer (1973), Plasmaspheric hiss, *J. Geophys. Res.*, *78*(10), 1581–1596, doi:10.1029/JA078i010p01581.

Thorne, R. M., B. Ni, X. Tao, R. B. Horne, and N. P. Meredith (2010), Scattering by chorus waves as the dominant cause of diffuse auroral precipitation, *Nature*, *467*, 943–946, doi:10.1038/nature09467.

Thorne, R. M., et al. (2013), Rapid local acceleration of relativistic radiation-belt electrons by magnetospheric chorus, *Nature*, *504*, 411–414, doi:10.1038/nature12889.

Wygant, J. R., et al. (2013), The electric field and waves instrument on the Radiation Belt Storm Probes mission, *Space Sci. Rev.*, *179*, 183–220, doi:10.1007/s11214-013-0013-7.